

Hierarchical Reinforcement Learning for the Dynamic VNE with Alternatives Problem

Ali Al Housseini*, Cristina Rottondi†, Omran Ayoub*

* University of Applied Sciences and Arts of Southern Switzerland, Lugano, Switzerland

† Politecnico di Torino, Turin, Italy

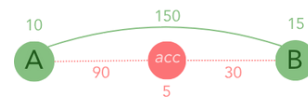
Abstract—Virtual Network Embedding (VNE) is a key enabler of network slicing, yet most formulations assume that each Virtual Network Request (VNR) has a fixed topology. Recently, VNE with Alternative topologies (VNEAP) was introduced to capture *malleable* VNRs, where each request can be instantiated using one of several functionally equivalent topologies that trade resources differently. While this flexibility enlarges the feasible space, it also introduces an additional decision layer, making dynamic embedding more challenging. This paper proposes HRL-VNEAP, a hierarchical reinforcement learning approach for VNEAP under dynamic arrivals. A high-level policy selects the most suitable alternative topology (or rejects the request), and a low-level policy embeds the chosen topology onto the substrate network. Experiments on realistic substrate topologies under multiple traffic loads show that naive exploitation strategies provide only modest gains, whereas HRL-VNEAP consistently achieves the best performance across all metrics. Compared to the strongest tested baselines, HRL-VNEAP improves acceptance ratio by up to 20.7%, total revenue by up to 36.2%, and revenue-over-cost by up to 22.1%. Finally, we benchmark against an MILP formulation on tractable instances to quantify the remaining gap to optimality and motivate future work on learning- and optimization-based VNEAP solutions.

I. INTRODUCTION

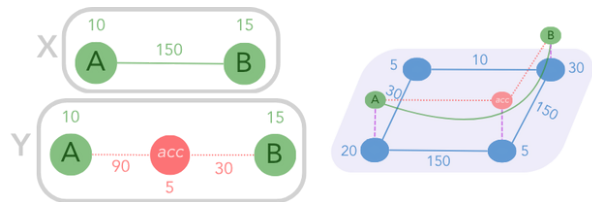
Network slicing is the paradigm of partitioning a shared physical network into multiple, logically isolated “slices,” each tailored to a tenant or service class with distinct requirements in terms of bandwidth, reliability, and security [1].

A central problem in network slicing is the *Virtual Network Embedding (VNE)* problem [2], which concerns the mapping of Virtual Network Requests (VNR) onto a physical network (also referred to as substrate network). In this context, each slice request, i.e., each VNR, specifies the virtual nodes and links it requires, along with their associated resource demands. The objective of the VNE is to allocate resources of the VNR (i.e., to embed the VNR) onto physical nodes and links while ensuring resource isolation and adherence to quality-of-service requirements (e.g., minimum bandwidth guarantees, maximum link latency, or packet loss limits). The embedding must also optimize system-level goals such as cost efficiency and resource utilization.

Most studies on the VNE problem assume that a VNR has a fixed topology [2], meaning that both the number of virtual nodes and the way they are interconnected by virtual links are *predetermined* and *immutable*. In other words, the structure of the virtual network graph is specified in advance to the embedding by the application. The orchestrator must then find an embedding that preserves this exact structure without



(a) Alternative topology 1



(b) VNEAP Example Scenario

Fig. 1: Alternative VN topologies, each showing a unique distribution of computational and bandwidth requirements, and a VNEAP example with two alternatives (X and Y) of a VNR.

omitting, rearranging, or substituting any part of the topology. This rigidity limits the flexibility of the embedding process, especially under resource constraints, since the orchestrator must satisfy the embedding of a fixed virtual topology without the option to choose a more suitable variant, or in other words, an *alternative*.

In a recent line of research, authors have introduced a novel variant of the VNE problem that leverages *malleable* VNRs [3], wherein each VNR can be realized through one of several alternative virtual network topologies (hereafter, we use the term *alternatives* to denote these alternative virtual network topologies). These alternatives are functionally equivalent but are implemented as different virtual networks, i.e., with different capacity and bandwidth requirements. From a practical standpoint, this aligns with the well-established practice in network virtualization of enabling flexible configurations. This flexibility creates a significant practical advantage as it allows the embedding algorithm to select a topology aligned with the current state of the Substrate Network (SN), thereby improving overall network efficiency [4].

To build an intuition, we provide the following illustrative example. Fig. 1a represents an application with two alternatives. The first (green) represents a Virtual Network (VN) consisting of two virtual nodes, A and B, each with a computational capacity of 10 and 15 units, respectively, and connected by a communication link requiring 150 bandwidth units. The second alternative (dotted in red) employs an *accumulator* (an intermediate node) between A and B requiring a computational

capacity of 5 units and two virtual links (A-accumulator, and accumulator-B) requiring 90 and 30 bandwidth units, respectively. While the accumulator increases compute requirements, it reduces the bandwidth requirements from 150 to 30. For instance, a video streaming service might have one topology that uses a compression function to greatly reduce bandwidth at the cost of additional CPU, and an alternative topology that skips compression to save CPU but uses more bandwidth [3].

Moreover, Fig. 1b illustrates how, depending on the objective, a specific alternative may be prioritized. Assume that the objective is to maximize the revenue-to-cost (R2C) ratio (Eq 1) [5]. While the embedding of each of the topologies is feasible (Fig 1a), $R2C(X) = \frac{175}{25+300} = 0.538$, whereas $R2C(Y) = \frac{150}{30+120} = 1$, thus Y results more favorable.

Compared to the classical VNE, VNEAP involves a joint optimization over both alternative selection and embedding decisions. It introduces an additional decision layer, as the orchestrator must first select one of the alternatives prior to embedding it onto the SN. This significantly enlarges the solution space, making traditional heuristic methods less effective and motivating the need for more intelligent, adaptive approaches. *Reinforcement Learning* (RL) has proven to be a promising solution paradigm for VNE, as it allows agents to learn embedding policies through experience. Yet, when extended to VNEAP, where the agent must both select an alternative and embed it, the action space becomes combinatorial, and flat RL policies struggle to scale.

In this work, we focus on the dynamic VNEAP problem, where VNRs arrivals are not known in advance, and the system must choose and embed an appropriate alternative. We address this with a hierarchical RL (HRL) framework: a high-level policy selects the topology alternative for each request, and a low-level policy embeds it onto the substrate. This separation shrinks the decision space and yields more focused learning. Our contributions can be summarized as follows:

- *HRL for VNEAP*: we design an HRL-based approach for the dynamic VNEAP problem, introducing a two-level policy structure that jointly handles topology selection and embedding.
- *MILP benchmark*: we develop a MILP formulation of VNEAP to provide an optimality reference for evaluating the HRL method.
- *Performance evaluation*: simulation results show improvements of up to 20.7% in acceptance ratio and 36.2% in average revenue compared with baselines.

II. RELATED WORK

The VNE problem has been widely studied through exact methods, heuristics, and learning-based approaches. Surveys such as Fischer *et al.* [2] and Wu *et al.* [6] summarize these directions, and recent work has focused in particular on RL and GNN-based models [7] to overcome the intractability of optimal formulations.

Hierarchical RL has also been explored in VNE to improve scalability by splitting the decision process. In VNE-HRL [8], a high-level agent selects which VNR to embed next, while a

low-level agent performs the actual mapping. HRL-ACRA [9] extends this idea to joint admission control and embedding, again using a high-level policy for admission decisions and a low-level policy for resource allocation. Both works show that hierarchical decomposition improves long-term reward and resource utilization over flat RL methods. These HRL approaches, however, target the classical VNE problem with pre-determined VNR topologies. None of them address alternative-topology selection, which substantially enlarges the decision space and cannot be reduced to, for instance, request ordering or the admission control problem.

As previously mentioned, VNE assumes a single fixed topology per request, which limits flexibility. Motivated by emerging applications that allow multiple feasible service or function configurations, the VNEAP formulation [3] explicitly introduces configurable alternative topologies for each VNR. Recent efforts have focused on handcrafted heuristics designed for narrow, static variants of VNEAP [3], while no learning-based method has addressed the dynamic VNEAP decision space. Our work fills this gap by introducing the first RL-based (specifically HRL) solution for dynamic VNEAP. Unlike prior RL methods for VNE, our formulation couples topology selection and embedding. Moreover, we provide the first empirical comparison against an MILP optimal baseline for online (dynamic) VNEAP, quantifying how close learning-based solutions can approach the true optimum.

III. DYNAMIC VNEAP

The VNEAP can be formulated as follows. *Given* i) a substrate network, modeled as a graph $\mathcal{G} = (\mathcal{N}_s, \mathcal{E}_s)$ where \mathcal{N}_s is the set of substrate nodes, and where $p \in \mathcal{N}_s$ has a finite amount of computing capacity denoted as c_p , and \mathcal{E}_s is the set of substrate links, and where $(u, v) \in \mathcal{E}_s$ has a bandwidth capacity b_{uv} ; *ii*) arriving VNRs defined by a set of *functionally equivalent* VN topologies (alternatives) where each request r in R has a set of alternatives $A_r = \{\mathcal{G}_{r,1}, \mathcal{G}_{r,2}, \dots, \mathcal{G}_{r,|A_r|}\}$, and $\mathcal{G}_{r,a} = (\mathcal{N}_{r,a}, \mathcal{E}_{r,a})$ represents a graph of virtual nodes and links, *decide* i) whether to embed a given VNR and in which alternative, and *ii*) the *embedding* onto the substrate network, *subject to* node placement, link routing, node couplings, capacity and bandwidths constraints, with the *objective* of maximizing revenue to cost ratio (R2C) (Eq 1) [10]. Note that a virtual node ($i \in \mathcal{N}_{r,a,i}$) represent VNFs and is represented by a CPU demand (capacity requirement) denoted as $c_{r,a,i}$, and virtual links represent communication between VNFs and have bandwidth demands $b_{r,a,i,j}$ for $(i, j) \in \mathcal{E}_{r,a}$. Moreover, we denote by τ_r the arrival time of a VNR and λ_r the holding time of a VNR (lifetime). Table I outlines sets, parameters and decision variables.

$$\begin{aligned}
\max \quad & \sum_{r \in \mathcal{R}} \sum_{a \in A_r} y_{r,a} \left(\sum_{i \in \mathcal{N}_{r,a}} c_{r,a,i} + \sum_{(i,j) \in \mathcal{E}_{r,a}} b_{r,a,i,j} \right) \\
& - \sum_{r \in \mathcal{R}} \sum_{a \in A_r} \sum_{i \in \mathcal{N}_{r,a}} \sum_{p \in \mathcal{N}_s} x_{r,a,i}^p c_{r,a,i} \\
& - \sum_{r \in \mathcal{R}} \sum_{a \in A_r} \sum_{(i,j) \in \mathcal{E}_{r,a}} \sum_{p \in \mathcal{N}_s} \sum_{q \in \mathcal{N}_s \setminus \{p\}} \sum_{P \in \rho_{pq}} w_{r,a,i,j}^P b_{r,a,i,j} \text{hops}(P)
\end{aligned} \tag{1}$$

Eq 1 represents the R2C objective. *Revenue* represents the fixed economic value of the requested virtual resources while *Cost* captures the actual consumption of physical resources, where the bandwidth demand is aggregated over every physical link (u, v) in the allocated path P with p and q corresponding to the substrate nodes where i and j are allocated, respectively.

The MILP is as follows:

$$\max \text{ Equation 1} \quad (2)$$

$$\text{s.t. } \sum_{a \in \mathcal{A}_r} y_{r,a} \leq 1 \quad \forall r \in \mathcal{R} \quad (3)$$

$$\sum_{p \in \mathcal{S}_{r,a,i}} x_{r,a,i}^p = y_{r,a} \quad \forall r, a, i \in \mathcal{N}_{r,a} \quad (4)$$

$$\sum_{i \in \mathcal{N}_{r,a}} x_{r,a,i}^p \leq y_{r,a} \quad \forall r, a, p \in \mathcal{N}_s \quad (5)$$

$$\sum_{p \in \mathcal{N}_s} \sum_{q \in \mathcal{N}_s \setminus \{p\}} \sum_{P \in \rho_{pq}} w_{r,a,ij}^P = y_{r,a} \quad \forall r, a, (i, j) \in \mathcal{E}_{r,a} \quad (6)$$

$$\sum_{q \in \mathcal{N}_s \setminus \{p\}} \sum_{P \in \rho_{pq}} w_{r,a,ij}^P \leq x_{r,a,i}^p \quad \forall r, a, (i, j) \in \mathcal{E}_{r,a}, p \in \mathcal{N}_s \quad (7)$$

$$\sum_{p \in \mathcal{N}_s \setminus \{q\}} \sum_{P \in \rho_{pq}} w_{r,a,ij}^P \leq x_{r,a,j}^q \quad \forall r, a, (i, j) \in \mathcal{E}_{r,a}, q \in \mathcal{N}_s \quad (8)$$

$$\sum_{r \in \mathcal{R}} \sum_{a \in \mathcal{A}_r} \sum_{i \in \mathcal{N}_{r,a}} \alpha_{r,t} c_{r,a,i} x_{r,a,i}^p \leq c_p \quad \forall p \in \mathcal{N}_s, \forall t \in T \quad (9)$$

$$\sum_{r \in \mathcal{R}} \sum_{a \in \mathcal{A}_r} \sum_{(i,j) \in \mathcal{E}_{r,a}} \alpha_{r,t} b_{r,a,ij} \sum_{\substack{p \\ q \neq p}} \sum_{\substack{q \\ P \in \rho_{pq} \\ (u,v) \in P}} w_{r,a,ij}^P \leq b_{uv} \quad \forall (u, v) \in \mathcal{E}_s, \forall t \in T \quad (10)$$

$$y_{r,a}, x_{r,a,i}^p, w_{r,a,ij}^P \in \{0, 1\} \quad (11)$$

Constr. 3 ensures that, for each VNR $r \in \mathcal{R}$, at most one alternative is selected. Constr. 4 ensures that each virtual node i of a selected alternative a for r (i.e., when $y_{r,a} = 1$), is mapped on exactly one substrate node $p \in \mathcal{S}_{r,a,i}$. Constr. 5 ensures that no two virtual nodes are co-located over the same substrate node. Constr. 6 is the link routing constraint, across all candidate endpoint pairs (p, q) and their candidate paths, exactly one path for each virtual (i, j) is selected, for the selected topology a . Constr. 7 and Constr. 8 are the source and destination endpoint coupling constraints (path must start where i is placed, and must end where j is placed, respectively). Constr. 9 ensures that at each time slot $t \in T$, the total active capacity demand placed on the substrate node p cannot exceed its maximum capacity c_p . We define an activity flag $\alpha_{r,t}$ that ensures that only VNRs alive at time t contribute, and is defined as:

$$\alpha_{r,t} = \begin{cases} 1 & \text{if } t \in \{\tau_r, \tau_r + 1, \dots, \tau_r + \lambda_r - 1\} \\ 0 & \text{otherwise} \end{cases} \quad (12)$$

Constr. 10 ensures link bandwidth constraint, where for each substrate link (u, v) and time t , sum of the bandwidth demands of all active virtual links that chose a path containing (u, v) , must not exceed the substrate link bandwidth $b_{u,v}$.

TABLE I: System model sets, parameters and variables

<i>Sets and Notations</i>	<i>Description</i>
$\mathcal{G} = (\mathcal{N}_s, \mathcal{E}_s)$	Undirected substrate network graph
$\mathcal{R} = \{r_1, \dots, r_n\}$	Set of virtual network requests
$\mathcal{A}_r = \{a_1, \dots, a_m\}$	Set of alternatives for VNR $r \in \mathcal{R}$
$\mathcal{G}_{r,a} = (\mathcal{N}_{r,a}, \mathcal{E}_{r,a})$	Virtual topology of alternative $a \in \mathcal{A}_r$
$T = \{1, \dots, T \}$	Set of time events
$\mathcal{S}_{r,a,i}$	Set of substrate nodes allowed to host virtual node $i \in \mathcal{N}_{r,a}$
ρ_{pq}	Set of simple substrate paths from p to q
P	Simple path $\in \rho_{pq}$
<i>Parameters</i>	<i>Description</i>
$c_p \in \mathbb{R}^+$	Capacity of node $p \in \mathcal{N}_s$
$b_{uv} \in \mathbb{R}^+$	Bandwidth of link $(u, v) \in \mathcal{E}_s$
$c_{r,a,i} \in \mathbb{R}^+$	Capacity demand of node $i \in \mathcal{N}_{r,a}$
$b_{r,a,ij} \in \mathbb{R}^+$	Bandwidth of link $(i, j) \in \mathcal{E}_{r,a}$
$\tau_r \in T$	Arrival time of request $r \in \mathcal{R}$
$\lambda_r \in \mathbb{R}^+$	Lifetime (holding) of request $r \in \mathcal{R}$
<i>Variables</i>	<i>Description</i>
$\alpha_{r,t} \in \{0, 1\}$	Active flag variable
$y_{r,a} \in \{0, 1\}$	Selection of alternative variable
$x_{r,a,i}^p \in \{0, 1\}$	Node placement variable
$w_{r,a,ij}^P \in \{0, 1\}$	Link routing variable

The standard VNE problem is known to be \mathcal{NP} -hard [2], and the introduction of malleable requests further expands the search space. Consequently, solving this ILP using exact solvers becomes computationally prohibitive for large problem instances. We explore RL-based approximation methods in the following section.

IV. HIERARCHICAL RL FOR VNEAP

Fig. 2 shows a schematic representation of HRL-VNEAP. VNRs arrive dynamically, and we cast the selection of alternatives (left) and resource allocation (right) as high-level (HL) and lower-level (LL) tasks, respectively. First, we encode the alternatives of current VNR and SN as the HL state where the agent's goal is to optimize the long-term benefits, including acceptance ratio and long-term revenue. Based on encoded information, the HL agent select a feasible action (i.e., an alternative) or rejects the request (proactive). The LL agent focuses on optimizing the placement of admitted alternative's nodes and edges. Given information from SN and the alternative, it performs a sequence of actions to embed virtual nodes over a set of feasible substrate nodes, then connect allocated nodes over a set of feasible paths. Once this process terminates, two separated rewards are returned to each agent. This process is repeated until all VNRs are processed.

A. High-level agent

The *high-level state space* S^{HL} is reported in Table II, and consists of aggregated encoded information from both \mathcal{G} and \mathcal{A}_r , including the topological description of each alternative (e.g., number of nodes/links, connectivity scores), requested resources (e.g., average capacity/bandwidth demand), and the lifetime of each VNR.

The *high-level action space* $A^{HL} = \{1, 2, \dots, |\mathcal{A}_r| + 1\}$ is designed as a multibinary variable that indicates the selected alternative, in addition to the action of rejecting a VNR (meaning that none of its alternatives is selected).

The *High-level reward* R^{HL} is designed to guide the agent to optimize the long-term resource efficiency. We define $r_t^{HL} \in R^{HL}$ as follows:

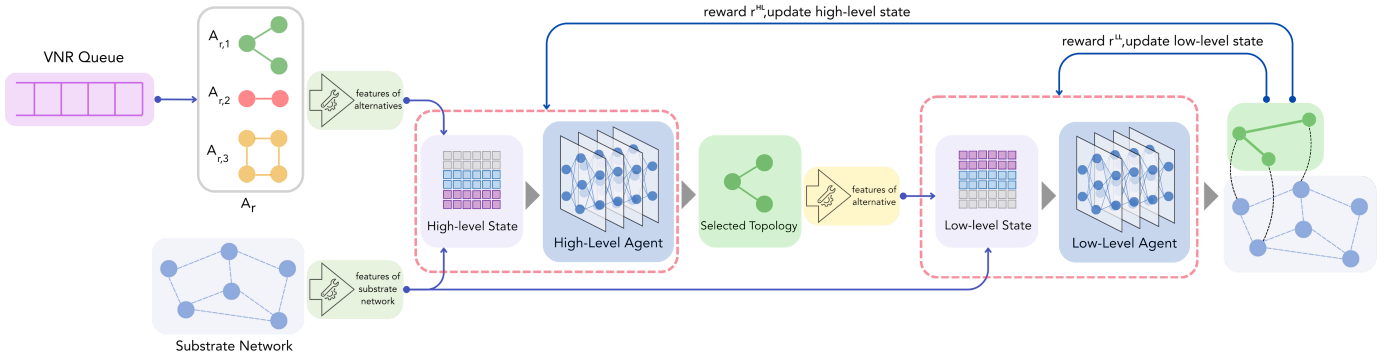


Fig. 2: Schematic representation of the proposed HRL architecture. HL agent observes the substrate and request features to select the optimal alternative. Subsequently, LL agent performs the embedding. Distinct reward signals (r^{HL} and r^{LL}) are used to update the respective policies.

$$r_t^{HL} = \begin{cases} \frac{Rev^2(a_t)}{Cost(a_t)} & \text{if alternative } a_t \text{ is embedded} \\ -\sigma & \text{if alternative } a_t \text{ is admitted but not embedded} \\ 0 & \text{otherwise} \end{cases} \quad (13)$$

Eq. 13 encourages the selection of alternatives that maximize the R2C ratio (Eq. 1), offering high positive reward value for successful embeddings. In case of failed embedding, the agent receives a negative reward. In case the agent's rejects a VNR, it is neither rewarded nor penalized.

B. Low-level agent

The *Low-level state space* S^{LL} shares the same encoded SN information with HL state, thus both agents operate on an identical view of the SN. Since the LL agent's objective is to perform the embedding of the chosen topology per VNR, it receives specific information of the requested resources (see Table II). To reflect the sequential nature of the embedding procedure, the state also includes specific context variables that indicate which component of the VNR is currently being embedded.

The *Low-level action space* A^{LL} is defined as $A^{LL} = \{1, 2, \dots, |\mathcal{N}_s|\}$ where each element corresponds to a specific

TABLE II: High-level and low-level states

	HL State	LL State
Substrate	Remaining capacity of sub. nodes	
	Load ratio of sub. nodes	
	Degree centrality of sub. nodes	
	Betweenness centrality of sub. nodes	
	Remaining bandwidth of sub. links	
	Load ratio of sub. links	
	Betweenness centrality of sub. links	
Virtual	Indexes of sub. nodes (masking)	
	Indexes of sub. links (masking)	
	Num nodes per alt.	Node cap. demands
	Num links per alt.	Link BW sums
	Avg cap. demand	Node degrees
Context	Avg BW demand	
	Avg path length	
	Avg connectivity	
	VNR Lifetime	Progress ratio
		Curr. node cap.
		Curr. node deg.

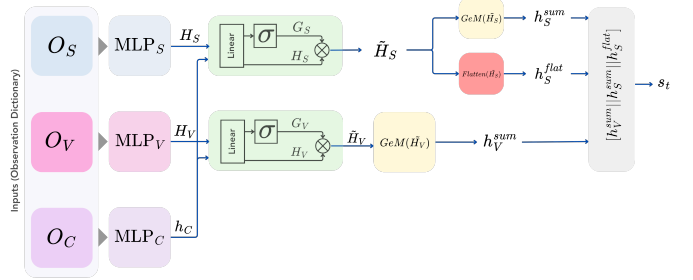


Fig. 3: Schematic overview of the policy design

node within the SN. At each step t , the agent will select an action $a_{t,k}^{LL}$ that corresponds to a substrate node where node k of alternative a_t^{HL} will be embedded. The allocation of links is done progressively via K-Shortest Path (K-SP) [11, 12].

The *Low-level reward* R^{LL} is multi-objective, to alleviate the sparse reward issue, leading to a more efficient exploration. We use the same reward design as in [11].

C. Policy Network Design

We now describe the customized design of our policy, illustrated in Fig 3. Both agents are trained by the Proximal Policy Optimization (PPO) method [13] using the same customized network. Let the raw observation dictionary at time t be partitioned into substrate features O_S , VNR features O_V (see Table II), and current embedding step context O_C . First, each input is projected into a shared latent feature space of dimension d_h through a dedicated (multi-layer perceptron) MLP encoder. This projection is essential to align the heterogeneous dimensions of different input modalities into a compatible latent space for uniform downstream processing. Let $H_S = \text{MLP}_S(O_S)$, $H_V = \text{MLP}_V(O_V)$, and $h_C = \text{MLP}_C(O_C)$ denote the encoded feature tensors for substrate, VNR, and context, respectively. Note that H_S and H_V typically represent sets of feature vectors corresponding to graph nodes or edges, whereas h_C is a single global context vector.

A core component of the architecture is the contextual gating mechanism, which dynamically modulates the resource features based on the current embedding phase. This explicit gating imposes a strong inductive bias, allowing the model to *filter* out irrelevant attributes early in the pipeline. Taking the

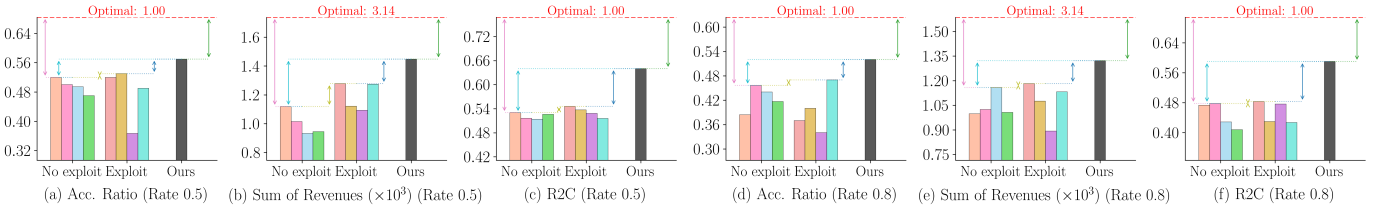
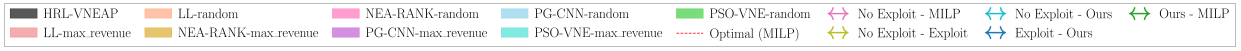


Fig. 4: Comparison of methods under arrival rates 0.5 and 0.8 on Atlanta Substrate Network

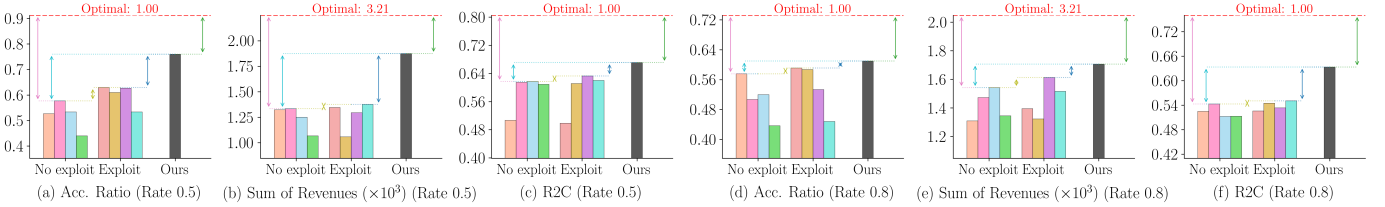


Fig. 5: Comparison of methods under arrival rates 0.5 and 0.8 on GEANT Substrate Network

substrate branch as an example, we first compute a tensor of importance weights, G_S as follows: The global context embedding h_C is broadcast and concatenated with the local node features H_S . This combined representation is passed through a linear layer and a sigmoid activation function $\sigma(\cdot)$ to map the values to the range $(0, 1)$.

$$G_S = \sigma(W_{GS}[H_S \parallel h_C]) \quad (14)$$

where $[\cdot \parallel \cdot]$ denotes concatenation, and W_{GS} are learnable parameters. Second, these generated importance weights are applied to the original feature embeddings. The final gated substrate representation, \tilde{H}_S , is obtained via the element-wise multiplication of the importance weights G_S and the original node values H_S :

$$\tilde{H}_S = H_S \odot G_S \quad (15)$$

This mechanism ensures that the network preserves the topological structure of H_S while scaling the magnitude of specific features according to their relevance to the current step context. An identical gating process is applied to the VNR branch to yield \tilde{H}_V .

Following gating, the features are aggregated to extract both global summaries and local descriptors. To obtain permutation-invariant representations of the graph structures, Generalized-Mean (GeM) pooling is applied [14]. We select GeM over standard average or max pooling because it employs a learnable parameter p , enabling the network to *adaptively* interpolate between capturing aggregate network capacity and identifying critical bottlenecks. For the substrate features, the summary vector h_S^{sum} is obtained as an output of this operation. A VNR summary h_V^{sum} is computed similarly. Crucially, to enable the actor head to distinguish between individual substrate nodes for action selection, the gated substrate features are also subjected to a flattening operation, yielding

$h_S^{flat} = \text{Flatten}(\tilde{H}_S)$. This hybrid approach preserves the node-specific spatial information required for *precise* action selection, while simultaneously providing the compact global context required for *efficient* value estimation. The final state representation s_t , which serves as input to the downstream policy and value heads, is constructed by concatenating these processed components: $s_t = [h_S^{sum} \parallel h_S^{flat} \parallel h_V^{sum}]$.

V. NUMERICAL RESULTS AND DISCUSSION

Experimental Settings We conduct experiments to mimic various realistic network systems. We adopt two topologies, Atlanta and GEANT [15] as physical networks. The capacity and bandwidth resources are uniformly generated within the range of [50,100] units as in [9]. In each simulation run, we randomly generate 30 VNRs, each with 4 possible alternatives. Additionally, resource demands of each VNR's node and link requirements are uniformly generated within the range of [0, 20] and [0, 50] units, respectively. The alternatives are generated by adding/removing nodes and links from a set of base topologies with a uniform probability within [0.4, 0.6]. The lifetime of each VNR is exponentially distributed with an average of 50 time units. To validate the performance of HRL-VNEAP, we compare it with the state-of-the-art heuristics: NEA-RANK [16], PSO-VNE [17], and RL baseline PG-CNN [18]. However, since these algorithms are for VNE (without alternatives), we test each with two high-level techniques: Random (where an alternative is randomly selected), and maximum revenue (alternative with largest revenue is returned) representing a heuristic technique for selection.

Numerical Results Figs. 4 and 5 report the performance of the various approaches on the Atlanta and GEANT topologies, respectively. For each topology, we show three metrics (acceptance ratio, sum of revenues, and R2C (Eq. 1) under two arrival rates ($\eta \in \{0.5, 0.8\}$). Within every subplot, approaches

are grouped into three categories: (i) *No exploit* (random alternative selection), which mimics “single-topology VNE” without leveraging alternatives; (ii) *Exploit*, where the HL exploitation rule is to select the alternative with the maximum revenue; and (iii) *Ours*, the proposed HRL-VNEAP method with a learned HL policy and a learned LL embedding policy. The horizontal dashed line corresponds to the optimal value given by the MILP formulation, while the vertical arrows annotate the gaps between the best approach in each category and, when relevant, the MILP optimum.

Impact of exploiting alternatives: Comparing the *No exploit* and *Exploit* groups isolates the effect of having alternatives but using a naive rule (max-revenue) to select alternatives. Overall, the gains are modest: In all scenarios, the best *Exploit* setting improves acceptance ratio by only **+1.9% to +9.2%**, total revenue by **+2.0% to +4.6%**, and R2C by only **+1.1% to +3.0%** over the best *No exploit* setting. This confirms that simply enlarging the decision space with alternatives is not sufficient; without a dedicated decision mechanism, performance remains close to classical VNE. In some cases, max-revenue selection is counterproductive, suggesting that max-revenue may pick alternatives that are harder to embed and degrade long-term throughput (e.g., on GEANT at $\eta = 0.5$ Fig 5(b), NEA-RANK drops from 1334 to 1058 in revenue).

Best-performing approach: HRL-VNEAP achieves the best performance in every scenario and across all metrics, indicating that it effectively exploits alternative topologies through learned HL selection and LL embedding. Compared to the flat baseline achieving best performance, HRL-VNEAP improves acceptance ratio by **+3.2% to +20.7%**, total revenue by **+5.9% to +36.2%**, and R2C by **+6.0% to +22.1%**. The gains also remain substantial over naive exploitation (max-revenue selection): e.g., on Atlanta at $\eta = 0.8$, acceptance increases from 0.470 (best *Exploit*) to 0.520 (**+10.6%**), while on GEANT at $\eta = 0.5$, revenue increases from 1376 to 1874 (**+36.2%**). These improvements suggest that the HL policy does not favor the highest instantaneous revenue alternative, but learns choices that preserve resources and improve long-term efficiency, as reflected by consistent R2C gains.

Optimality Gap (HRL-VNEAP vs. MILP): The dashed line shows the offline MILP optimum, which jointly optimizes over the *entire* request set (including arrival times and lifetimes) with full future knowledge. In contrast, HRL-VNEAP operates online. Under this stricter setting, HRL-VNEAP achieves acceptance ratios of 0.52–0.76 versus an MILP acceptance of 1.0, revenues of $1.322\text{--}1.874 \times 10^3$ versus 3.21×10^3 (Atlanta) / 3.14×10^3 (GEANT), and R2C of 0.590–0.671 versus 1.00. Equivalently, the remaining gaps to MILP are about **24–48%** in acceptance, **40–59%** in total revenue, and **33–41%** in R2C across the tested scenarios.

Effect of load and topology: Increasing the arrival rate from $\eta = 0.5$ to $\eta = 0.8$ increases stress and degrades performance for all methods (lower acceptance and typically lower R2C). However, the relative ranking remains stable and HRL-VNEAP remains best under both loads; for instance on Atlanta at $\eta = 0.8$ Fig 4(d)(e)(f), HRL-VNEAP achieves 0.520

acceptance and 1322 revenue, while the best baseline reaches 1183 revenue. Across network topologies, GEANT (Fig 5) consistently allows higher performance than Atlanta (e.g., HRL-VNEAP acceptance 0.760 vs. 0.570 at $\eta = 0.5$), which is consistent with higher embedding flexibility in GEANT. Overall, the results reinforce that alternatives alone provide limited benefit unless exploited by an appropriate decision mechanism, and that HRL-VNEAP remains particularly effective under high load when resource scarcity makes alternative selection critical.

VI. CONCLUSION

In this paper, we proposed HRL-VNEAP, a HRL framework for VNE with alternatives problem (VNEAP). We designed a customized and efficient policy that enables long-term planning and adaptive decisions. Results across an extensive set of experiments verify the effectiveness of HRL-VNEAP and demonstrate that HRL-VNEAP outperforms baselines and shows promising results for achieving near optimal. Future work includes enriching the alternative-selection space and narrowing the gap to optimality.

REFERENCES

- [1] Z. S. et al, “An overview of network slicing for 5g,” *IEEE Wireless Communications*, 2019.
- [2] F. et al, “Virtual network embedding: A survey,” *IEEE Communications Surveys & Tutorials*, 2013.
- [3] K. et al, “The power of alternatives in network embedding,” in *IEEE INFOCOM 2025*, 2025.
- [4] M. F. Bari, S. R. Chowdhury, R. Ahmed, and R. Boutaba, “On orchestrating virtual network functions,” in *2015 11th international conference on network and service management (CNSM)*. IEEE, 2015, pp. 50–56.
- [5] Y. M. et al, “Rethinking virtual network embedding: substrate support for path splitting and migration,” *ACM SIGCOMM Computer Communication Review*, 2008.
- [6] W. S. et al, “Ai-empowered virtual network embedding: A comprehensive survey,” *IEEE Communications Surveys & Tutorials*, 2025.
- [7] H.-K. L. et al, “Reinforcement learning-based virtual network embedding: A comprehensive survey,” *ICT Express*, 2023.
- [8] C. J. et al, “Vne-hrl: A proactive virtual network embedding algorithm based on hierarchical reinforcement learning,” *IEEE Transactions on Network and Service Management*, 2021.
- [9] W. T. et al, “Joint admission control and resource allocation of virtual network embedding via hierarchical deep reinforcement learning,” *IEEE Transactions on Services Computing*, 2023.
- [10] C. M. et al, “Polyvine: Policy-based virtual network embedding,” *IEEE Transactions on Network and Service Management*, 2012.
- [11] Y. Z. et al, “Automatic virtual network embedding: A deep reinforcement learning approach with graph convolutional networks,” *IEEE Journal on Selected Areas in Communications*, 2020.
- [12] C. X. et al, “Virtual network embedding through topology-aware node ranking,” *ACM SIGCOMM Computer Communication Review*, 2011.
- [13] S. J. et al, “Proximal policy optimization algorithms,” *arXiv preprint arXiv:1707.06347*, 2017.
- [14] R. F. et al, “Fine-tuning cnn image retrieval with no human annotation,” *IEEE transactions on pattern analysis and machine intelligence*, 2018.
- [15] S. O. et al, “SNDlib 1.0—Survivable Network Design Library,” in *Proceedings of the 3rd International Network Optimization Conference (INOC 2007)*, Spa, Belgium, 2007.
- [16] F. W. et al, “Node essentiality assessment and distributed collaborative virtual network embedding in datacenters,” *IEEE Transactions on Parallel and Distributed Systems*, 2023.
- [17] J. C. et al, *VNE-HPSO Virtual Network Embedding Algorithm Based on Hybrid Particle Swarm Optimization*. Springer Singapore, 2021.
- [18] Z. P. et al, “Reinforcement learning assisted bandwidth aware virtual network resource allocation,” *IEEE Transactions on Network and Service Management*, 2022.